

## Electron-Neutrino Angular Correlation in the Beta Decay of Neon-19\*

MYRON L. GOOD AND EUGENE J. LAUER  
*Radiation Laboratory, University of California, Berkeley, California*

(Received July 23, 1956)

The distribution in kinetic energy of the recoil ions associated with beta rays of known energy in the beta decay of  $\text{Ne}^{19}$  has been measured. For the coefficient  $\lambda$  in the theoretical distribution in the cosine of the angle between the outgoing electron and neutrino,  $[1 + \lambda(v/c) \cos\theta]$ , we find a value of  $\lambda = +0.14 \pm 0.13$ , suggesting that the Fermi component of the beta decay interaction is scalar.

### INTRODUCTION

MEASUREMENTS of the electron-neutrino angular correlation coefficient for the beta decay of  $\text{He}^6$  have shown that the Gamow-Teller component of the beta-decay interaction is tensor.<sup>1,2</sup> In the experiment reported here, the angular correlation coefficient is measured for the decay of  $\text{Ne}^{19}$  (which can have a mixture of Gamow-Teller and Fermi-type interactions) in order to determine whether the Fermi component is scalar or vector. When an atom undergoes beta decay, there are three quantities that can be measured (if the neutrino is not detected)—the energy of the beta particle, the energy of the recoil ion, and the angle  $\phi$  between these two. In the experimental arrangement used for this experiment, the distribution in kinetic energy of the recoil ions associated with beta rays of known energy was measured. Because of the geometry of the experiment and the relatively high energy of the beta particles that were used, all possible angles  $\phi$  were accepted. The beta-ray energy and recoil energy are sufficient to completely determine the decay, and thus to permit calculation of  $\theta$  (the angle between the directions of the beta ray and the neutrino) for each event. The beta-particle energy was measured with a scintillation counter and the associated recoil-ion kinetic energy was determined by measuring the time delay needed after the beta pulse for the recoil ion to traverse a known drift distance and hit the first dynode of an electron-multiplier tube.

Previous experiments<sup>3,4</sup> have indicated that the Fermi component of the beta-decay interaction is scalar, and our results strengthen this conclusion.

### PRODUCTION OF NEON-19

$\text{Ne}^{19}$  was produced by the  $(p,n)$  reaction on  $\text{F}^{19}$ , by bombarding tightly packed 0.001-inch-thick lathe turnings of Teflon with about  $10^{-8}$  ampere of 32-Mev protons from the UCRL 40-foot linear accelerator. The active gas diffused in an approximately  $10^{-4}$ -mm Hg

vacuum from the bombardment target through a liquid nitrogen-cooled charcoal trap (which pumps air and all impurity activities except He and Ne) and through about 15 feet of 1-inch-diameter copper tubing to the recoil chamber and counting apparatus outside the shielding wall.

Decay curves taken with the beta counter and with the recoil-ion counter both indicated a single activity, with a half-life in agreement with the published value of  $18.5 \pm 0.5$  seconds.<sup>5</sup> The purity of the activity, as judged from the decay curve, was better than 99%.

### RECOIL CHAMBER AND COUNTERS

Figure 1 shows the recoil chamber, the beta scintillation counter, and the recoil-ion counter. A good event was a  $\text{Ne}^{19}$  beta decay which: (a) occurred inside the

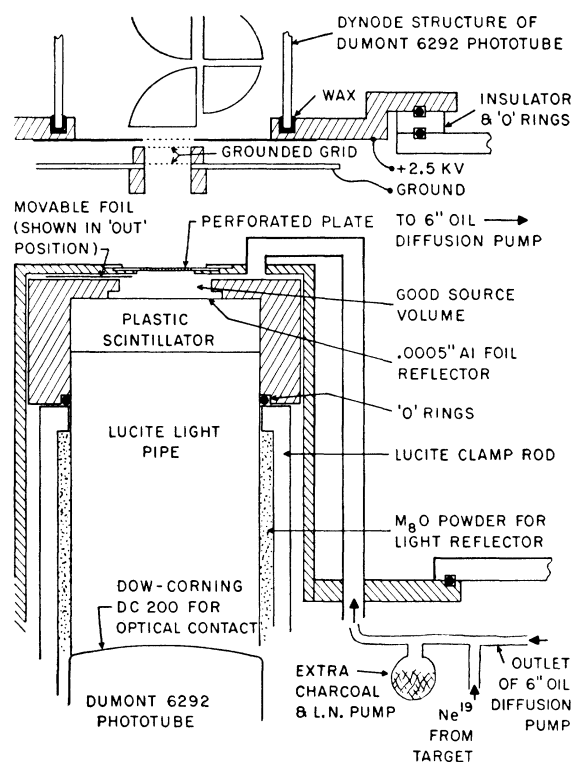


Fig. 1. Vacuum chamber, recoil counter, and beta-ray scintillation counter.

\* This work was done under the auspices of the U. S. Atomic Energy Commission.

<sup>1</sup> J. S. Allen and W. K. Jentschke, *Phys. Rev.* **89**, 902(A) (1953).

<sup>2</sup> B. M. Rustad and S. L. Ruby, *Phys. Rev.* **97**, 991 (1955).

<sup>3</sup> W. P. Alford and D. R. Hamilton, *Phys. Rev.* **95**, 1351 (1954).

<sup>4</sup> Maxson, Allen, and Jentschke, *Phys. Rev.* **97**, 109 (1955).

<sup>5</sup> G. Schrank and J. R. Richardson, *Phys. Rev.* **86**, 248 (1952).

good source volume (between the foil on the scintillator and the movable foil), (b) sent the recoil ion through one of the holes of the perforated plate in a direction to pass through the grid-covered hole in front of the recoil-ion counter, and (c) had a beta-particle energy  $\geq 1.4$  Mev. Betas of this high energy have two or more times the momentum of the associated neutrino, and so go within  $30^\circ$  of the opposite direction from the recoil ion. Because of the geometry, such beta rays were certain to hit the scintillator, for all values of  $\theta$ .

The perforated plate was an aluminum plate 0.015 in. thick with 0.006-in. diameter closely spaced holes drilled through in a circular region, centered on the axis of the counters. This plate offered impedance to the flow of  $\text{Ne}^{19}$  gas from the good source volume to the drift space, so that the diffusion pump, which pumped on the drift space and discharged into the good source volume, could maintain an active gas density about 1/100 as great in the drift space as in the good source volume. (This was determined by pressure measurements using stable Ne.)

The charcoal pump maintained the air pressure at about  $3 \times 10^{-6}$  mm Hg in the drift space and about  $2 \times 10^{-4}$  mm Hg in the good source volume.

The movable foil was used to subtract the background of delayed coincidences due to decays in the drift space. With the foil "open," decays in the good source volume and the drift space could cause delayed coincidences; with the foil "closed," delayed coincidences due to decays in the good source volume were prevented because the ions could not penetrate the 0.0005-in. thick aluminum foil. However, decays in the drift space could cause delayed coincidences, since their beta rays could penetrate the foil. A gas conductance path, large compared with the gas conductance of the perforated plate, was provided around the movable foil so that the density distribution of  $\text{Ne}^{19}$  atoms was nearly the same with foil open or closed. The small change in the density distribution was measured by using stable Ne at low pressures, and the data were corrected for this.

The energy scale and energy resolution of the beta counter were determined by measuring the pulse-height distribution of Compton-electron pulses from the 1.28-Mev  $\gamma$  rays of  $\text{Na}^{22}$ . The position of the Compton edge gives the energy scale, while the width of the edge may be used to determine the energy resolution. A more direct calibration was obtained by measuring the pulse-height distribution produced by monoenergetic electrons from a small magnetic spectrograph. This agreed well with the  $\text{Na}^{22}$  method. The more convenient  $\text{Na}^{22}$  method was therefore used for occasional checks of resolution and energy scale as the experiment proceeded. The full width at half maximum of the pulse-height distribution due to monoenergetic particles was about 20% of the mean energy.

These calibrations did not measure effects due to counting of the  $\text{Ne}^{19}$  annihilation quanta. These were

approximately taken into account by calculation in preparing the theoretical curves of Fig. 2, and proved to be quite small.

The recoil-ion counter consisted of the electron-multiplier structure of a Dumont 6292 phototube, obtained by cutting off the photocathode end of the glass envelope. The cylindrical envelope was then waxed into a metal groove. After evacuation, the dynodes were reactivated by heating to a dull red with an induction heating coil. A potential of 2.5 kilovolts was applied between the grounded grid (Fig. 1) and the first dynode.<sup>6</sup> A fluorothene plug and socket was used on the recoil counter to minimize leakage pulses. The recoil-ion counter was tested with positive ions or electrons that could be obtained by heating a thin tungsten filament in the drift space. The pulse-height discriminator was set at  $\frac{1}{3}$  the maximum height of the pulses due to a single electron leaving the first dynode (as determined by bombarding it with ions of very low energy). Typical recoil-ion pulse sizes were much larger than this. The sensitivity of the counter to recoil energy of the recoil ions was not measured, but should be small because the number of secondary electrons released by ions in this energy range is proportional to the ion energy, while the energy of the ions after acceleration varied only from 2.5 kilovolts for a recoil of zero initial kinetic energy, to 2.7 kv for a recoil of 200-ev initial kinetic energy.

After amplification, the pulses from the beta counter and from the recoil counter were sent to a mixing circuit,

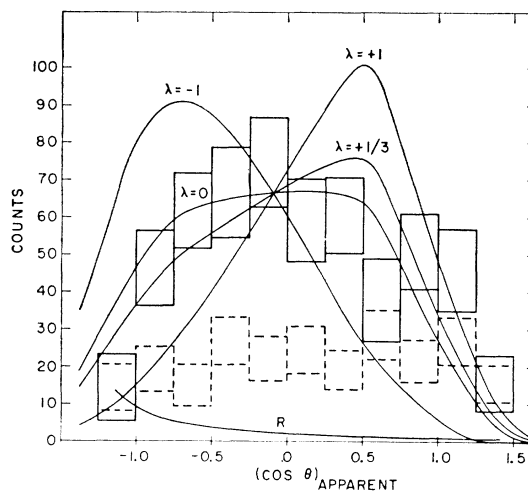


FIG. 2. Distribution in  $\cos\theta$  of  $\text{Ne}^{19}$  beta-decay events. Solid rectangles give the measured distribution in  $\cos\theta$ , with random background and foil-closed background subtracted. The dotted rectangles are the foil-closed background with foil-closed randoms subtracted, and the solid curve labeled  $R$  is the foil-open random background. The height of the rectangles is two times the standard deviation. The solid curves are theoretical, with instrumental resolution folded in, for various values of  $\lambda$ .

<sup>6</sup> This grid was a double grid, especially designed to minimize leakage of the high accelerating field into the field-free drift space.

the output of which triggered the sweep of a Tektronix 517 oscilloscope if the recoil pulse was between  $-0.6$  and  $+3.4$  microseconds after the beta pulse. The amplified pulses were also delayed and applied to the two vertical plates of the oscilloscope. A 35-mm strip camera photographed the pairs of pulses. The pulses were displayed in a film viewer, and for each pair of pulses the height of the beta pulse was measured to give the energy of the beta particle, and the time delay of the recoil pulse after the beta pulse was measured to give the energy of the recoil ion. The random-coincidence background was measured by a separate scaler and mixer circuit which counted the recoil pulses that occurred between 40 and 80 microseconds after each beta pulse.

### THEORETICAL CURVES

The distribution in  $\cos\theta$  may be determined in a simple way from the beta-ray energy  $W$  and the recoil energy  $E$ . If  $p$  is the beta-ray momentum,  $q$  the neutrino momentum, and  $R$  the recoil momentum, then by applying the law of cosines to the momentum triangle for the decay, we have

$$R^2 = p^2 + q^2 + 2pq \cos\theta,$$

$$E = \frac{R^2}{2M} = \frac{p^2 + q^2}{2M} + \frac{pq}{M} \cos\theta = a + b \cos\theta$$

( $M$  = recoil-ion mass),

where  $a$ ,  $b$  are essentially constants for fixed beta-ray energy. The recoil energy is thus a linear function of  $\cos\theta$ .

The theoretical distribution expected is of the form

$$f(\theta)d\Omega = \left(1 + \lambda \frac{v}{c} \cos\theta\right) d\Omega.$$

Here  $v$  and  $c$  are velocities of the beta ray and of light. For such an expression, the distribution in recoil energy, for a fixed beta-ray energy, has a simple form. It is different from zero only between an upper and a lower recoil energy limit (at which limits  $\cos\theta = \pm 1$ ). The distribution of recoil energies is a linear function of recoil energy between these limits. The upper and lower recoil energy limits depend, however, on the beta-ray energy.

In preparing theoretical curves, the recoil-energy distributions for each beta-ray energy are first averaged over the energy resolution of the beta counter, and over the distribution in drift distances from different parts of the good source volume, to yield a distribution in apparent recoil energy for fixed beta-counter pulse size.

A convenient way to combine the data taken at different beta-ray energies is to replot the theoretical curves *versus* the apparent value of  $\cos\theta$ , rather than

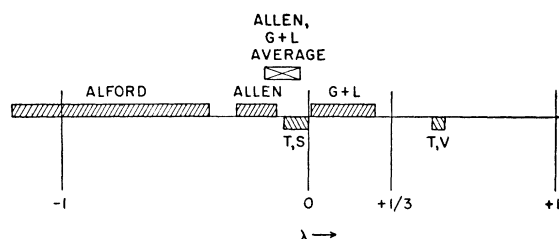


FIG. 3. Determinations of  $\lambda$  for  $\text{Ne}^{19}$ .

recoil energy. Since  $\cos\theta$  varies between the same limits for all curves, the contributions from different beta-ray energies may simply be added to yield a theoretical distribution in the apparent value of  $\cos\theta$ . (Since the apparent recoil energy can exceed the true energy, because of instrumental resolution, the apparent value of  $\cos\theta$  can exceed the limits on  $\cos\theta$  of  $\pm 1$ .) The theoretical curves of Fig. 2 were obtained in this way. The curve for  $\lambda = 0$  becomes a rectangle with edges at  $\cos\theta = \pm 1$  for infinitely good instrumental resolution, and therefore its deviation from this form measures the resolution of the apparatus.

### RESULTS

The experiment was run for approximately five 16-hour days, alternating between "foil open" and "foil closed" about every 25 minutes. After the film was read to give the beta energy and recoil-ion time delay for each pair of pulses, the data were divided into eleven equal beta-energy windows between 1.4 and 1.9 Mev. Each of these sets of data was analyzed separately by calculating the recoil-ion delay times for the edges of  $\cos\theta$  windows, each 0.25 unit wide, for a decay in which the beta particle had the mean energy for that beta window, and counting the number of delay times that fell in each of these  $\cos\theta$  windows. Finally, the data for the eleven beta-energy windows were added, to form a distribution in  $\cos\theta$  including all the data. This procedure was carried out for all the "foil open" data and for all the "foil closed" data, the random count as deduced from the random scaler was subtracted from each, and then the "foil closed" data were subtracted from the "foil open" data. Figure 2 shows the measured distribution, and also shows the "foil closed" background and random background.

A least-squares fit of the theoretical curve to the data of Fig. 2 gives  $\lambda = +0.14 \pm 0.13$ . For the tensor-vector interaction, we have  $+\frac{1}{3} \leq \lambda \leq +1$  and for the tensor-scalar combination,  $-1 \leq \lambda \leq +\frac{1}{3}$ , so that the result given suggests that the Fermi component of the beta-decay interaction is scalar, in agreement with previous determinations.<sup>3,4</sup> None of the three determinations of  $\lambda$  overlap, but a weighted average of our result with that of Allen *et al.*<sup>4</sup> agrees well with the expected value for tensor plus scalar of  $-0.05 \pm 0.05$ , and neither is in

serious disagreement with it (Fig. 3). (The expected values for  $T$ ,  $S$  and  $T$ ,  $V$  are arrived at by using the  $\text{Ne}^{19}$  and  $\text{O}^{14}$   $ft$  values.)<sup>6,7</sup>

It has been pointed out to us by Dr. J. S. Allen that our apparatus may have been partly sensitive to neutral recoils. Since the detection efficiency for neutrals would be expected to increase with increasing kinetic energy of the neutral atom, this effect, if present, would bias our data toward more positive values of  $\lambda$ . The con-

clusion that the Fermi component of the beta interaction is scalar is unaffected, since it depends on  $\lambda$ 's being less than  $+\frac{1}{3}$ .

#### ACKNOWLEDGMENTS

The authors are pleased to acknowledge valuable discussions with Dr. Luis Alvarez, assistance during the early stages of the experiment by Dr. Arthur Schelberg, untiring service by the linear accelerator operating crew, and aid in calculating the theoretical distribution by Keith Johnston and Charles Stableford.

<sup>6</sup> S. R. de Groot and H. A. Tolhoek, *Physica* **16**, 456 (1950).

<sup>7</sup> J. B. Gerhart, *Phys. Rev.* **95**, 288 (1954).

## Thermal-Neutron Coherent Scattering Amplitudes of Thallium and Osmium\*

LEROY HEATON AND S. S. SIDHU  
*Argonne National Laboratory, Lemont, Illinois*

(Received September 17, 1956)

The value of coherent scattering amplitudes, coherent cross sections, and scattering cross sections for bound nucleus for thallium and osmium are given.

### INTRODUCTION

THE coherent neutron scattering amplitude of thallium reported previously<sup>1</sup> was determined from the total neutron cross-section curve of the polycrystalline compound  $\text{TlBr}$  obtained as a function of neutron energy. The curve contained cross section peaks in the energy range of 0.001 to 1.0 electron volt, that were due to coherent scattering of neutrons from various crystalline planes. From analysis of the curve the magnitude of the scattering amplitude was found to be  $(0.75 \pm 0.08) \times 10^{-12}$  cm and was based on the then known value<sup>2</sup> of the scattering amplitude of bromine as  $0.56 \times 10^{-12}$  cm. The latter value has been shown to be low.<sup>3</sup> The compound  $\text{TlBr}$  has therefore, been restudied with improved neutron diffraction techniques and the coherent scattering amplitude of thallium has been measured by a comparison with that of nickel as a standard. The coherent scattering amplitude of osmium has been also measured by the same method for the first time.

### EXPERIMENTAL

Neutron diffraction patterns were made from cylindrical samples by the techniques described elsewhere<sup>4</sup> and the scattering amplitudes were calculated by the

method described by Shull and Wollen.<sup>5,6</sup> This method is based upon the measurement of the integrated intensities of the diffraction peaks of a sample whose crystal structure is either known or determined first, and which contains the element for which the scattering amplitude is to be determined. For a powdered cylindrical sample the integrated intensity,  $P_{hkl}/P_0$  from a set of  $hkl$  planes is given by the expression:

$$\frac{P_{hkl}}{P_0} = K^2 \frac{\rho'}{\rho_0} N_c^2 \frac{j_{hkl}}{\sin\theta \sin^2\theta} F_{hkl}^2(0) e^{-2W} A_{hkl}, \quad (1)$$

where  $P_0$  is the intensity of the incident monochromatic beam, and  $K$  is a constant of the experiment and includes the geometry of the spectrometer as well as the neutron wavelength and the volume of the sample in the beam. The value of  $K$  is determined by using a nickel powder sample as a standard. The value of  $\rho'/\rho_0$ , the "packing" of the samples, was determined from the measured density  $\rho'$  of the samples and the true or the solid specimen density  $\rho_0$ , which was calculated from the atomic weights of the elements composing the crystal and its known crystal structure.  $N_c$ , the number of unit cells per cubic centimeter, was calculated from the reciprocal of the volume of the unit cell of the structure.  $F_{hkl}(0)$  is the structure factor when  $\sin\theta/\lambda=0$ , and is a function of the nuclear scattering amplitudes; and  $W$  is the Debye-Waller temperature factor. The absorption correction factor  $A_{hkl}$

\* Work performed under the auspices of the U. S. Atomic Energy Commission.

<sup>1</sup> Winsberg, Meneghetti, and Sidhu, *Phys. Rev.* **75**, 975 (1949).

<sup>2</sup> E. Fermi and L. Marshall, *Phys. Rev.* **71**, 666 (1947).

<sup>3</sup> C. G. Shull and E. O. Wollan, in *Solid State Physics*, edited by F. Seitz and D. Turnbull (Academic Press, Inc., New York, 1956), Vol. 2, p. 137.

<sup>4</sup> Sidhu, Heaton, and Zaubers, *Acta Cryst.* **9**, 607 (1956).

<sup>5</sup> C. G. Shull and E. O. Wollan, *Phys. Rev.* **81**, 527 (1951).

<sup>6</sup> E. O. Wollan and C. G. Shull, *Phys. Rev.* **73**, 822 (1948).